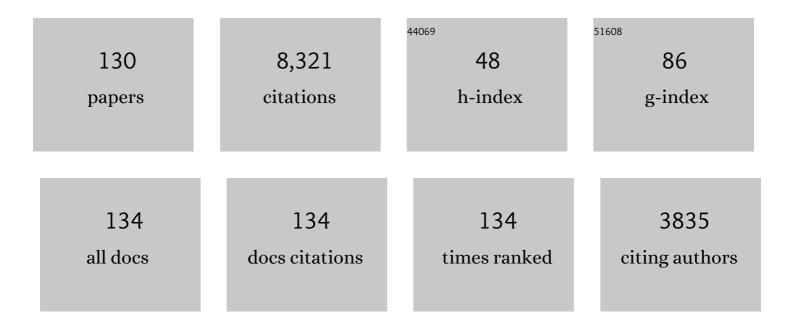
List of Publications by Year in descending order

Source: https://exaly.com/author-pdf/8943376/publications.pdf Version: 2024-02-01



#	Article	IF	CITATIONS
1	Frictional and Lithological Controls on Shallow Slow Slip at the Northern Hikurangi Margin. Geochemistry, Geophysics, Geosystems, 2022, 23, .	2.5	16
2	Deformation Process and Mechanism of the Frontal Megathrust at the Nankai Subduction Zone. Geochemistry, Geophysics, Geosystems, 2022, 23, .	2.5	1
3	Spatial Variation of Shallow Stress Orientation Along the Hikurangi Subduction Margin: Insights From Inâ€ <del>S</del> itu Borehole Image Logging. Journal of Geophysical Research: Solid Earth, 2022, 127, .	3.4	5
4	Seafloor overthrusting causes ductile fault deformation and fault sealing along the Northern Hikurangi Margin. Earth and Planetary Science Letters, 2022, 593, 117651.	4.4	6
5	Variable In Situ Stress Orientations Across the Northern Hikurangi Subduction Margin. Geophysical Research Letters, 2021, 48, e2020GL091707.	4.0	8
6	Asymmetric Brittle Deformation at the PÄpaku Fault, Hikurangi Subduction Margin, NZ, IODP Expedition 375. Geochemistry, Geophysics, Geosystems, 2021, 22, e2021GC009662.	2.5	4
7	P―and Sâ€Wave Velocities of Exhumed Metasediments From the Alaskan Subduction Zone: Implications for the In Situ Conditions Along the Megathrust. Geophysical Research Letters, 2021, 48, e2021GL094511.	4.0	7
8	Implications of basement rock alteration in the Nankai Trough, Japan for subduction megathrust slip behavior. Tectonophysics, 2020, 774, 228275.	2.2	11
9	The State of Stress on the Fault Before, During, and After a Major Earthquake. Annual Review of Earth and Planetary Sciences, 2020, 48, 49-74.	11.0	49
10	Physical Properties and Gas Hydrate at a Near‧eafloor Thrust Fault, Hikurangi Margin, New Zealand. Geophysical Research Letters, 2020, 47, e2020GL088474.	4.0	20
11	The Role of Deformation Bands in Dictating Poromechanical Properties of Unconsolidated Sand and Sandstone. Geochemistry, Geophysics, Geosystems, 2020, 21, e2020GC009143.	2.5	1
12	Slip-rate-dependent friction as a universal mechanism for slow slip events. Nature Geoscience, 2020, 13, 705-710.	12.9	51
13	Evolution of Elastic and Mechanical Properties During Fault Shear: The Roles of Clay Content, Fabric Development, and Porosity. Journal of Geophysical Research: Solid Earth, 2020, 125, e2019JB018612.	3.4	12
14	Coupled Evolution of Deformation, Pore Fluid Pressure, and Fluid Flow in Shallow Subduction Forearcs. Journal of Geophysical Research: Solid Earth, 2020, 125, e2019JB019101.	3.4	16
15	Mechanical and hydrological effects of seamount subduction on megathrust stress and slip. Nature Geoscience, 2020, 13, 249-255.	12.9	74
16	Friction experiments under in-situ stress reveal unexpected velocity-weakening in Nankai accretionary prism samples. Earth and Planetary Science Letters, 2020, 538, 116180.	4.4	15
17	A method for determining absolute ultrasonic velocities and elastic properties of experimental shear zones. International Journal of Rock Mechanics and Minings Sciences, 2020, 130, 104306.	5.8	4
18	Slow slip source characterized by lithological and geometric heterogeneity. Science Advances, 2020, 6, eaay3314.	10.3	95

DEMIAN M SAFFER

#	Article	IF	CITATIONS
19	The Effects of Shear Strain, Fabric, and Porosity Evolution on Elastic and Mechanical Properties of Clayâ€Rich Fault Gouge. Journal of Geophysical Research: Solid Earth, 2019, 124, 10968-10982.	3.4	19
20	Mixed deformation styles observed on a shallow subduction thrust, Hikurangi margin, New Zealand. Geology, 2019, 47, 872-876.	4.4	33
21	Effects of temperature on the frictional behavior of material from the Alpine Fault Zone, New Zealand. Tectonophysics, 2019, 762, 17-27.	2.2	10
22	Introduction to Theme 2: Probing the Dynamic Earth and Assessing Geohazards. Oceanography, 2019, 32, 78-79.	1.0	0
23	Future Opportunities in Scientific Ocean Drilling: Natural Hazards. Oceanography, 2019, 32, 135-135.	1.0	0
24	Pressure and Stress Prediction in the Nankai Accretionary Prism: A Critical State Soil Mechanics Porosityâ€Based Approach. Journal of Geophysical Research: Solid Earth, 2018, 123, 1089-1115.	3.4	22
25	Changes in Physical Properties of the Nankai Trough Megasplay Fault Induced by Earthquakes, Detected by Continuous Pressure Monitoring. Journal of Geophysical Research: Solid Earth, 2018, 123, 1072-1088.	3.4	10
26	Connections between subducted sediment, pore-fluid pressure, and earthquake behavior along the Alaska megathrust. Geology, 2018, 46, 299-302.	4.4	47
27	Mechanics of Foldâ€∎ndâ€Thrust Belts Based on Geomechanical Modeling. Journal of Geophysical Research: Solid Earth, 2018, 123, 4454-4474.	3.4	19
28	In Situ Permeability and Scale Dependence of an Active Accretionary Prism Determined From Crossâ€Borehole Experiments. Geophysical Research Letters, 2018, 45, 6935-6943.	4.0	10
29	Frictional Mechanics of Slow Earthquakes. Journal of Geophysical Research: Solid Earth, 2018, 123, 7931-7949.	3.4	54
30	Installation of a High Sensitivity Ocean Borehole Strainmeter in the Nankai Trough Under Severe Sea Current Conditions. Marine Technology Society Journal, 2018, 52, 128-137.	0.4	0
31	Permeability Evolution of Propped Artificial Fractures in Green River Shale. Rock Mechanics and Rock Engineering, 2017, 50, 1473-1485.	5.4	21
32	The action of water films at Ãscales in the Earth: Implications for the Nankai subduction system. Earth and Planetary Science Letters, 2017, 463, 266-276.	4.4	13
33	Strength and deformation behavior of the Shimanto accretionary complex across the Nobeoka thrust. Island Arc, 2017, 26, e12192.	1.1	4
34	Recurring and triggered slow-slip events near the trench at the Nankai Trough subduction megathrust. Science, 2017, 356, 1157-1160.	12.6	222
35	In Situ Stress and Pore Pressure in the Deep Interior of the Nankai Accretionary Prism, Integrated Ocean Drilling Program Site C0002. Geophysical Research Letters, 2017, 44, 9644-9652.	4.0	20
36	Mapping fluids to subduction megathrust locking and slip behavior. Geophysical Research Letters, 2017, 44, 9337-9340.	4.0	20

DEMIAN M SAFFER

#	Article	IF	CITATIONS
37	Tsunamigenic structures in a creeping section of the Alaska subduction zone. Nature Geoscience, 2017, 10, 609-613.	12.9	65
38	The postearthquake stress state on the Tohoku megathrust as constrained by reanalysis of the JFAST breakout data. Geophysical Research Letters, 2017, 44, 8294-8302.	4.0	20
39	Links between sediment consolidation and Cascadia megathrust slip behaviour. Nature Geoscience, 2017, 10, 954-959.	12.9	60
40	Links between clay transformation and earthquakes along the Costa Rican subduction margin. Geophysical Research Letters, 2017, 44, 7725-7732.	4.0	9
41	In situ stress magnitude and rock strength in the Nankai accretionary complex: a novel approach using paired constraints from downhole data in two wells. Earth, Planets and Space, 2016, 68, .	2.5	13
42	Boron desorption and fractionation in <scp>S</scp> ubduction <scp>Z</scp> one <scp>F</scp> ore Arcs: Implications for the sources and transport of deep fluids. Geochemistry, Geophysics, Geosystems, 2016, 17, 4992-5008.	2.5	7
43	Distribution of stress state in the Nankai subduction zone, southwest Japan and a comparison with Japan Trench. Tectonophysics, 2016, 692, 120-130.	2.2	45
44	Experimental constraints on the relationship between clay abundance, clay fabric, and frictional behavior for the <scp>C</scp> entral <scp>D</scp> eforming <scp>Z</scp> one of the <scp>S</scp> an <scp>A</scp> ndreas <scp>F</scp> ault. Geochemistry, Geophysics, Geosystems, 2016, 17, 3865-3881.	2.5	11
45	Laboratory observations of slow earthquakes and the spectrum of tectonic fault slip modes. Nature Communications, 2016, 7, 11104.	12.8	301
46	Nearâ€field observations of an offshore <i>M<sub>w</sub></i> 6.0 earthquake from an integrated seafloor and subseafloor monitoring network at the Nankai Trough, southwest Japan. Journal of Geophysical Research: Solid Earth, 2016, 121, 8338-8351.	3.4	71
47	In situ stress magnitudes at the toe of the Nankai Trough Accretionary Prism, offshore Shikoku Island, Japan. Journal of Geophysical Research: Solid Earth, 2016, 121, 1202-1217.	3.4	22
48	Breakdown pressure and fracture surface morphology of hydraulic fracturing in shale with H 2 O, CO 2 and N 2. Geomechanics and Geophysics for Geo-Energy and Geo-Resources, 2016, 2, 63-76.	2.9	119
49	Frictional properties of the active San Andreas Fault at SAFOD: Implications for fault strength and slip behavior. Journal of Geophysical Research: Solid Earth, 2015, 120, 5273-5289.	3.4	82
50	Evolution of permeability across the transition from brittle failure to cataclastic flow in porous siltstone. Geochemistry, Geophysics, Geosystems, 2015, 16, 2980-2993.	2.5	9
51	The impact of splay faults on fluid flow, solute transport, and pore pressure distribution in subduction zones: A case study offshore the <scp>N</scp> icoya <scp>P</scp> eninsula, <scp>C</scp> osta <scp>R</scp> ica. Geochemistry, Geophysics, Geosystems, 2015, 16, 1089-1104.	2.5	18
52	The permeability of active subduction plate boundary faults. Geofluids, 2015, 15, 193-215.	0.7	39
53	Permeability and pressure measurements in Lesser Antilles submarine slides: Evidence for pressureâ€driven slowâ€slip failure. Journal of Geophysical Research: Solid Earth, 2015, 120, 7986-8011.	3.4	16
54	Downdip variations in seismic reflection character: Implications for fault structure and seismogenic behavior in the Alaska subduction zone. Journal of Geophysical Research: Solid Earth, 2015, 120, 7883-7904.	3.4	54

4

#	Article	IF	CITATIONS
55	Stiffness evolution of granular layers and the origin of repetitive, slow, stick-slip frictional sliding. Granular Matter, 2015, 17, 447-457.	2.2	30
56	Strength characteristics of Japan Trench borehole samples in the high-slip region of the 2011 Tohoku-Oki earthquake. Earth and Planetary Science Letters, 2015, 412, 35-41.	4.4	68
57	The frictional, hydrologic, metamorphic and thermal habitat of shallow slow earthquakes. Nature Geoscience, 2015, 8, 594-600.	12.9	216
58	Fluid budgets along the northern Hikurangi subduction margin, New Zealand: the effect of a subducting seamount on fluid pressure. Geophysical Journal International, 2015, 202, 277-297.	2.4	62
59	The roles of quartz and water in controlling unstable slip in phyllosilicate-rich megathrust fault gouges. Earth, Planets and Space, 2014, 66, .	2.5	30
60	Hydraulic and acoustic properties of the active Alpine Fault, New Zealand: Laboratory measurements on DFDP-1 drill core. Earth and Planetary Science Letters, 2014, 390, 45-51.	4.4	50
61	Frictional properties of low-angle normal fault gouges and implications for low-angle normal fault slip. Earth and Planetary Science Letters, 2014, 408, 57-65.	4.4	30
62	Consolidation state of incoming sediments to the Nankai Trough subduction zone: Implications for sediment deformation and properties. Geochemistry, Geophysics, Geosystems, 2014, 15, 2821-2839.	2.5	17
63	Stress State in the Largest Displacement Area of the 2011 Tohoku-Oki Earthquake. Science, 2013, 339, 687-690.	12.6	112
64	Slip weakening as a mechanism for slow earthquakes. Nature Geoscience, 2013, 6, 468-472.	12.9	121
65	Shear zones in clay-rich fault gouge: A laboratory study of fabric development and evolution. Journal of Structural Geology, 2013, 51, 206-225.	2.3	121
66	Analysis of normal fault populations in the Kumano forearc basin, Nankai Trough, Japan: 2. Principal axes of stress and strain from inversion of fault orientations. Geochemistry, Geophysics, Geosystems, 2013, 14, 1973-1988.	2.5	27
67	Apparent overconsolidation of mudstones in the Kumano Basin of southwest Japan: Implications for fluid pressure and fluid flow within a forearc setting. Geochemistry, Geophysics, Geosystems, 2013, 14, 1023-1038.	2.5	15
68	In situ stress and pore pressure in the Kumano Forearc Basin, offshore SW Honshu from downhole measurements during riser drilling. Geochemistry, Geophysics, Geosystems, 2013, 14, 1454-1470.	2.5	23
69	Analysis of normal fault populations in the Kumano Forearc Basin, Nankai Trough, Japan: 1. Multiple orientations and generations of faults from 3â€D coherency mapping. Geochemistry, Geophysics, Geosystems, 2013, 14, 1989-2002.	2.5	42
70	Experimental evidence linking slip instability with seafloor lithology and topography at the Costa Rica convergent margin. Geology, 2013, 41, 891-894.	4.4	49
71	Determination of stress state in deep subsea formation by combination of hydraulic fracturing in situ test and core analysis: A case study in the IODP Expedition 319. Journal of Geophysical Research: Solid Earth, 2013, 118, 1203-1215.	3.4	25
72	Elevated pore pressure and anomalously low stress in regions of low frequency earthquakes along the Nankai Trough subduction megathrust. Geophysical Research Letters, 2012, 39, .	4.0	110

#	Article	IF	CITATIONS
73	Scale dependence of <i>inâ€situ</i> permeability measurements in the Nankai accretionary prism: The role of fractures. Geophysical Research Letters, 2012, 39, .	4.0	19
74	Fluid budgets of subduction zone forearcs: The contribution of splay faults. Geophysical Research Letters, 2012, 39, .	4.0	20
75	Frictional properties and sliding stability of the San Andreas fault from deep drill core. Geology, 2012, 40, 759-762.	4.4	88
76	Effects of smectite to illite transformation on the frictional strength and sliding stability of intact marine mudstones. Geophysical Research Letters, 2012, 39, .	4.0	49
77	Comparison of frictional strength and velocity dependence between fault zones in the Nankai accretionary complex. Geochemistry, Geophysics, Geosystems, 2011, 12, .	2.5	79
78	Heat advection by groundwater flow through a heterogeneous permeability crust: A potential cause of scatter in surface heat flow near Parkfield, California. Journal of Geophysical Research, 2011, 116, .	3.3	16
79	Mechanical characterization of slope sediments: Constraints on in situ stress and pore pressure near the tip of the megasplay fault in the Nankai accretionary complex. Geochemistry, Geophysics, Geosystems, 2011, 12, n/a-n/a.	2.5	24
80	Hydrogeology and Mechanics of Subduction Zone Forearcs: Fluid Flow and Pore Pressure. Annual Review of Earth and Planetary Sciences, 2011, 39, 157-186.	11.0	428
81	Consolidation and overpressure near the seafloor in the Ursa Basin, Deepwater Gulf of Mexico. Earth and Planetary Science Letters, 2011, 305, 11-20.	4.4	57
82	Submarine landslide potential near the megasplay fault at the Nankai subduction zone. Earth and Planetary Science Letters, 2011, 312, 453-462.	4.4	28
83	Weakness of the San Andreas Fault revealed by samples from the active fault zone. Nature Geoscience, 2011, 4, 251-254.	12.9	235
84	On the relation between fault strength and frictional stability. Geology, 2011, 39, 83-86.	4.4	278
85	Presentâ€day principal horizontal stress orientations in the Kumano forearc basin of the southwest Japan subduction zone determined from IODP NanTroSEIZE drilling Site C0009. Geophysical Research Letters, 2010, 37, .	4.0	76
86	Elevated fluid pressure and extreme mechanical weakness of a plate boundary thrust, Nankai Trough subduction zone. Geology, 2009, 37, 679-682.	4.4	170
87	A critical evaluation of crustal dehydration as the cause of an overpressured and weak San Andreas Fault. Earth and Planetary Science Letters, 2009, 284, 447-454.	4.4	22
88	Evaluation of in situ smectite dehydration as a pore water freshening mechanism in the Nankai Trough, offshore southwest Japan. Geochemistry, Geophysics, Geosystems, 2009, 10, .	2.5	47
89	Pore pressure development beneath the décollement at the Nankai subduction zone: Implications for plate boundary fault strength and sediment dewatering. Journal of Geophysical Research, 2009, 114, .	3.3	56
90	Frictional behavior of materials in the 3D SAFOD volume. Geophysical Research Letters, 2009, 36, .	4.0	75

#	Article	IF	CITATIONS
91	Effect of thermal refraction on heat flow near the San Andreas Fault, Parkfield, California. Journal of Geophysical Research, 2009, 114, .	3.3	14
92	Clay fabric intensity in natural and artificial fault gouges: Implications for brittle fault zone processes and sedimentary basin clay fabric evolution. Journal of Geophysical Research, 2009, 114, .	3.3	80
93	Frictional and hydrologic properties of clayâ€rich fault gouge. Journal of Geophysical Research, 2009, 114, .	3.3	342
94	Evaluation of factors controlling smectite transformation and fluid production in subduction zones: Application to the Nankai Trough. Island Arc, 2008, 17, 208-230.	1.1	93
95	12. Fault Friction and the Upper Transition from Seismic to Aseismic Faulting. , 2007, , 346-369.		30
96	Effect of hydration state on the frictional properties of montmorillonite-based fault gouge. Journal of Geophysical Research, 2007, 112, .	3.3	154
97	Hydrogeologic responses to three-dimensional temperature variability, Costa Rica subduction margin. Journal of Geophysical Research, 2006, 111, .	3.3	76
98	An evaluation of factors influencing pore pressure in accretionary complexes: Implications for taper angle and wedge mechanics. Journal of Geophysical Research, 2006, 111, .	3.3	83
99	Fluid expulsion and overpressure development during initial subduction at the Costa Rica convergent margin. Earth and Planetary Science Letters, 2005, 233, 361-374.	4.4	31
100	Permeability of underthrust sediments at the Costa Rican subduction zone: Scale dependence and implications for dewatering. Geophysical Research Letters, 2005, 32, .	4.0	27
101	Critically pressured free-gas reservoirs below gas-hydrate provinces. Nature, 2004, 427, 142-144.	27.8	167
102	Along-strike variations in underthrust sediment dewatering on the Nicoya margin, Costa Rica related to the updip limit of seismicity. Geophysical Research Letters, 2004, 31, .	4.0	58
103	Re-evaluation of heat flow data near Parkfield, CA: Evidence for a weak San Andreas Fault. Geophysical Research Letters, 2004, 31, .	4.0	44
104	Pore pressure development and progressive dewatering in underthrust sediments at the Costa Rican subduction margin: Comparison with northern Barbados and Nankai. Journal of Geophysical Research, 2003, 108, .	3.3	112
105	Topographically driven groundwater flow and the San Andreas heat flow paradox revisited. Journal of Geophysical Research, 2003, 108, .	3.3	36
106	Anisotropy of electrical conductivity record of initial strain at the toe of the Nankai accretionary wedge. Journal of Geophysical Research, 2003, 108, .	3.3	49
107	Fluid flow at the toe of convergent margins: interpretation of sharp pore-water geochemical gradients. Earth and Planetary Science Letters, 2003, 213, 261-270.	4.4	35
108	Comparison of smectite- and illite-rich gouge frictional properties: application to the updip limit of the seismogenic zone along subduction megathrusts. Earth and Planetary Science Letters, 2003, 215, 219-235.	4.4	476

#	Article	IF	CITATIONS
109	Escape of methane gas through sediment waves in a large methane hydrate province. Geology, 2002, 30, 467.	4.4	58
110	Porosity loss within the underthrust sediments of the Nankai accretionary complex: Implications for overpressures. Geology, 2002, 30, 19.	4.4	122
111	Hydrologic controls on the morphology and mechanics of accretionary wedges. Geology, 2002, 30, 271.	4.4	104
112	New insights into deformation and fluid flow processes in the Nankai Trough accretionary prism: Results of Ocean Drilling Program Leg 190. Geochemistry, Geophysics, Geosystems, 2001, 2, n/a-n/a.	2.5	189
113	Laboratory results indicating complex and potentially unstable frictional behavior of smectite clay. Geophysical Research Letters, 2001, 28, 2297-2300.	4.0	134
114	Smectite diagenesis, pore-water freshening, and fluid flow at the toe of the Nankai wedge. Earth and Planetary Science Letters, 2001, 194, 97-109.	4.4	115
115	Updip limit of the seismogenic zone beneath the accretionary prism of southwest Japan: An effect of diagenetic to low-grade metamorphic processes and increasing effective stress. Geology, 2001, 29, 183.	4.4	405
116	Inferred pore pressures at the Costa Rica subduction zone: implications for dewatering processes. Earth and Planetary Science Letters, 2000, 177, 193-207.	4.4	95
117	Fluid flow paths in the Middle America Trench and Costa Rica margin. Geology, 2000, 28, 679-682.	4.4	5
118	Fluid budgets at convergent plate margins: Implications for the extent and duration of fault-zone dilation. Geology, 1999, 27, 1095.	4.4	45
119	Episodic fluid flow in the Nankai accretionary complex: Timescale, geochemistry, flow rates, and fluid budget. Journal of Geophysical Research, 1998, 103, 30351-30370.	3.3	152
120	Expedition 358 summary. Proceedings of the International Ocean Discovery Program, 0, , .	0.0	10
121	Expedition 372B/375 summary. Proceedings of the International Ocean Discovery Program, 0, , .	0.0	20
122	Site U1518. Proceedings of the International Ocean Discovery Program, 0, , .	0.0	16
123	Data report: consolidation characteristics of sediments from Sites C0002, C0006, and C0007, IODP Expeditions 315 and 316, NanTroSEIZE Stage 1. Proceedings of the Integrated Ocean Drilling Program Integrated Ocean Drilling Program, 0, , .	1.0	20
124	Data report: consolidation, permeability, and fabric of sediments from the Nankai continental slope, IODP Sites C0001, C0008, and C0004. Proceedings of the Integrated Ocean Drilling Program Integrated Ocean Drilling Program, 0, , .	1.0	17
125	Data report: permeability and consolidation behavior of sediments from the northern Japan Trench subduction zone, IODP Site C0019. Proceedings of the Integrated Ocean Drilling Program Integrated Ocean Drilling Program, 0, , .	1.0	2
126	Expedition 348 summary. Proceedings of the Integrated Ocean Drilling Program Integrated Ocean Drilling Program, 0, , .	1.0	18

DEMIAN M SAFFER

#	Article	IF	CITATIONS
127	Site C0002. Proceedings of the Integrated Ocean Drilling Program Integrated Ocean Drilling Program, 0, , .	1.0	28
128	Data Report: Permeability and Consolidation Properties of Subducting Sediments off Costa Rica, ODP Leg 205. , 0, , .		10
129	IODP Expedition 319, NanTroSEIZE Stage 2: First IODP Riser Drilling Operations and Observatory Installation Towards Understanding Subduction Zone Seismogenesis. Scientific Drilling, 0, 10, 4-13.	0.6	7
130	Site C0024. Proceedings of the International Ocean Discovery Program, 0, , .	0.0	1